Equilibria for Adsorption of Phosphates on OH-Type Strongly Basic Ion Exchanger

Hiroyuki Yoshida and Wilmer A. Galinada
Dept. of Chemical Engineering, Osaka Prefecture University, Sakai 599-8531, Japan

The equilibrium isotherms for adsorption of phosphate ions using an OH-type, strongly basic ion exchanger, DIAION SA10A, were studied experimentally and the results appeared technically feasible. Four different types of phosphate ions, H_3PO_4, $H_2PO_4^{-}$, HPO_4^{2-}, and PO_4^{3-}, were used. In all the systems considered, the experimental adsorption isotherms showed a high amount of phosphate adsorption. Moreover, differences in the adsorption behaviors were observed. These differences were highly influenced by the pH of the equilibrated solutions. The ion-exchange reaction models were then proposed. By the mass action law, the theoretical equations for the adsorption isotherms were derived and the unknown experimental equilibrium constants were determined. These equilibrium models were able to correlate the experimental data well and explained the peculiarities in the obtained experimental adsorption isotherms.

Introduction

Phosphates are very important basic materials to many industries. They are used in very large quantities in the manufacture of fertilizers, detergents, water softeners, baking powders, processed food and drinks, and other important phosphate-based products. In the automotive and appliance industries, phosphating is an important metal-surface treatment process in the production of iron and steel to affect the appearance, surface hardness, electrical properties, and some corrosion resistance of the metal (Kirk et al., 1981; Elvers et al., 1990). Inevitably, the consumption of phosphate-bearing products in households and the massive utilization of concentrated phosphate solutions in the industries are producing large amounts of phosphate-bearing wastes. Although these wastes are conventionally treated, they are hardly recovered, and eventually discharged into the municipal and industrial wastewater streams.

Most countries in the world are primarily import-dependent on the raw materials of phosphates for industrial production processes. However, the supply of high-grade phosphate rocks, the raw material of choice for producing high-purity phosphoric acid by the wet process, is rapidly decreasing (Considine, 1984). In addition, there have been alarming reports that deposits of high-grade phosphate ores would likely be depleted in the next few decades. Thus, it is very important to develop a production process of phosphates from phosphate-utilizing industrial processes and phosphate-containing wastewater systems as alternative resources of phosphates to prevent such global exhaustion of high-grade phosphate ores in the very near future.

It was reported that phosphate concentrations in the first- and second-step treated water from sewage treatment facilities are in the ranges of $0.9-1.5\times10^{-2}$ mole L^{-1} and $2.0\times10^{-5}-2.3\times10^{-3}$ mole L^{-1}, respectively (Ogawa, 1980) and the phosphate concentrations used in the phosphating process are in the range of 0.05–1 mole L^{-1} (Asahara, 1976; Aotani, 1966). If these phosphates are successfully and economically recovered, then they could become viable alternative resources of high-grade phosphates.

Extensive studies on the effective treatment of phosphates in phosphate-containing wastewater systems have been previously conducted (Zhao and Sengupta, 1996, 1998; Sengupta and Zhao, 2000; Tanasheva et al., 1992; Boki and Tanada, 1987). The two most commonly used processes in phosphate removal from municipal and industrial wastewater are the chemical precipitation and the biological treatment processes (Jenkins and Hermanowicz, 1991; Stensel, 1991). These processes essentially transfer phosphates from the liquid to the sludge that needs to be hauled and dumped elsewhere. The concentrated phosphates in the sludge, are, thus, entirely wasted and just become an environmental hazard. Moreover,

---

Correspondence concerning this article should be addressed to H. Yoshida.

the ion-exchange process using ion exchangers has also been identified as a treatment method for phosphate removal (Boki and Tanada, 1987). The process development for the removal and recovery of phosphorus from wastewater using enhanced activated alumina has been published in a series by Urano and Tachikawa (1991). They reported that the enhanced activated alumina can adsorb various inorganic phosphorus species in a pH range from 4–7. And recently, Sengupta and Zhao (2000) have patented their research work in the United States on the selective removal of phosphates and chromates from contaminated water by ion-exchange using a new class of sorbent. Their sorbent is basically a copper-loaded chelating ion exchanger with styrene-divinylbenzene polymer matrix designed to effectively remove divalent phosphate ion (HPO_4^{2-}) at above-neutral pH. As reported, their results appeared technically feasible. However, in actual municipal and industrial wastewater, where the pH widely varies, the existence of other forms of phosphate ions such H_3PO_4, $H_2PO_4^-$, PO_4^{3-} or other species is inevitable. In such a case, their sorbent becomes technically ineffective unless those phosphate species are first converted into divalent form and then the pH of the solution is adjusted to above the neutral range for adsorption. Therefore, it is very important to use an adsorbent that can adsorb various species of phosphates and that can work effectively in a wide range of pH. In addition, the authors further acknowledged that their discovery is not bounded by any particular theory to support the underlying sorption mechanism of their sorbent.

In this experimental study, an OH-type strongly basic anion exchanger with styrene-divinylbenzene polymer matrix, DIAION SA10A, was used to effectively remove four different forms of phosphate ions, namely, H_3PO_4, $H_2PO_4^-$, HPO_4^{2-}, and PO_4^{3-} in aqueous media at each pH range where the species exist, respectively. The superiority of DIAION SA10A as an effective adsorbent over two other commercial ion exchangers, chitosan bead and chitosan fiber, was also confirmed beforehand. Since there are no existing fundamental studies on the ion-exchange mechanism of these phosphate ions using the OH-type strongly basic anion exchanger, it is, therefore, necessary to first understand the underlying basic ion-exchange mechanism of these ions onto this type of ion-exchanger to clearly elucidate their exchange behavior, and in order to establish working equilibrium models that could eventually lead to the development of an adsorption-recovery technology for phosphates.

The phosphate compounds considered are H_3PO_4, NaH_2PO_4, Na_2HPO_4, and Na_3PO_4, which are technically and commercially the most important group of phosphorus compounds except for the acid itself (Elvers et al., 1991). By assuming that phosphate ions are adsorbed by the neutralization reaction and ion-exchange reaction with the counterion OH^-, and by applying the mass action law, the theoretical equations for the adsorption isotherms are derived and the unknown experimental equilibrium constants are determined. In addition, these derived equilibrium models will be further tested by considering other competing ions such as chloride, sulfate, calcium, nitrate, to determine the commercial feasibility of the OH-type anion exchanger. This aspect and the studies on the rate of adsorption using the shallow-bed method and the fixed-bed column will also be reported subsequently.

Experimental Studies

The phosphate compounds H_3PO_4 and $Na_3PO_4 \cdot 12H_2O$ were purchased from Nacalai Tesque Inc., Japan, and the compounds $NaH_2PO_4 \cdot 2H_2O$ and $Na_2HPO_4 \cdot 12H_2O$ were obtained from Kishida Reagents Chemicals, Japan. The phosphate compounds and other chemicals used were all special grade and used as received.

The resin particles were properly conditioned to obtain the OH^--form. A sufficient amount of resin particles was sieved at a particle-size range of 24–28 mesh. After complete moistening with deionized water, the resin particles (about 500 cm^3) were transferred inside a glass column with an internal diameter of 3.5 cm and with a height of 100 cm, and then sufficiently filled with deionized water. The conditioning started with an acid washing. A 2,000-cm^3, 0.05-$kmol \cdot m^{-3}$ HCl aqueous solution was flowed through the column. Then the pH of the solution at the outlet of the column was measured. The same process was repeated for 0.07, 0.10, 0.15, 0.20, 0.30, 0.50, 0.70 and 1.0 $kmol \cdot m^{-3}$ HCl aqueous solution concentrations. The process was terminated when the inlet and the outlet pH of the solution were already equal. The resin particles were then sufficiently rinsed with deionized water. Next, a series of 2,000 cm^3 NaOH solution with concentrations similar to the HCl solutions just mentioned was flowed through the column. Also, the pH at the inlet and the outlet of the column was measured continuously until equality was attained. The resin particles were again sufficiently washed with deionized water until the outlet and the inlet pH became equal. Finally, the resin particles were dried under vacuum. Dry resin particles are practically more accurate and easier to weigh than wet ones.

The experimental systems and conditions of this equilibrium study are summarized in Table 1. The initial feed concentrations of all adsorbates were set at ranges of 0.01, 0.05 and 0.10 $kmol \cdot m^{-3}$. These phosphate concentrations are within the range of those in the first-step treated water and phosphating bath. The feed concentration of H_3PO_4 solution was accurately determined by the neutralization-titration method using 1.0 $kmol \cdot m^{-3}$ NaOH aqueous solution as the titrant. On the other hand, the feed concentrations of NaH_2PO_4, Na_2HPO_4, and Na_3PO_4 aqueous solutions were all accurately determined by flame analysis using the Atomic Absorption Spectrophotometer (SAS 7500A, Seiko Instruments Inc., Japan). A phosphate standard solution of 0.10-mg $PO_4^{3-} \cdot mL^{-1}$ (Japanese Industrial Standards, 1996) was used in all calibrations.

The equilibrium adsorption isotherms of phosphates were measured by the batch method. The various measured weights of the resin particles were contacted with the adsorbate solutions for all concentration ranges and the samples were placed inside the incubator with a constant stirring at an operating

Table 1. Experimental Systems and Conditions

Resin	Type of Resin	Adsorbates $Used_{(aq)}$	Feed Conc. ($kmol \cdot m^{-3}$)	Temp. (K)
DIAION SA10A (Gel Type)	OH^-	H_3PO_4	0.10, 0.05, 0.01	298
		NaH_2PO_4	0.10, 0.05, 0.01	
		Na_2HPO_4	0.10, 0.05, 0.01	
		Na_3PO_4	0.10, 0.05, 0.01	

temperature of 298 ± 0.5 K. The ion-exchange equilibria were attained in four days. After equilibration, the pH of the equilibrated solutions was measured with a pH meter (F-22, Horiba Ltd., Japan). The phosphate ion concentration in the equilibrated solutions was determined in the UV-Visible Recording Spectrophotometer (UV-160A, Shimadzu Corp., Japan) using the molybdenum blue method (ascorbic acid reduction). The resin-phase concentration of phosphate ion q [mole·(kg dry resin)$^{-1}$] was calculated according to Eq. 1

$$q = \frac{(C_o - C_T)V}{W} \tag{1}$$

where C_o and C_T [kmol·m^{-3}] are the initial and the final phosphate concentrations in the liquid phase, respectively; V [m^3] is the volume of the adsorbate solution; and, W [kg] is the weight of the resin particles. All experiments were carried out at 298 K.

Ion Exchanger

The ion exchanger used in this experimental study is a commercial strongly basic ion exchanger, DIAION SA10A (Mitsubishi Chemical Co., Japan). The network is made of styrene-divinylbenzene, and its functional group is quaternary ammonium (type I). The experimental physical properties are listed in Table 2. The concentration of the amino group in the adsorbent phase (total ion-exchange capacity of the resin) was determined by measuring the equilibrium isotherm for adsorption of HCl. The reaction may be expressed by the following acid/base neutralization reaction

$$\text{R-OH}^- + \text{HCl} \overset{K_{\text{HCl}}}{\rightleftharpoons} \text{R-Cl}^- + \text{H}_2\text{O} \tag{2}$$

where R-OH$^-$ denotes the strongly basic resin. Applying the mass action law to Eq. 2, the Langmuir Eq. 3 is derived

$$q_{\text{HCl}} = \frac{K_{\text{HCl}} Q C_{\text{HCl}}}{1 + K_{\text{HCl}} C_{\text{HCl}}} \tag{3}$$

The saturation capacity Q [mole·(kg dry resin)$^{-1}$] and the equilibrium constant K_{HCl} [mole·(kg dry resin)$^{-1}$] were determined from Eq. 4, which was transformed from Eq. 3

$$C_{\text{HCl}} = -\frac{1}{K_{\text{HCl}}} + Q\frac{C_{\text{HCl}}}{q_{\text{HCl}}} \tag{4}$$

The solid line in Figure 1 shows the Langmuir isotherm obtained by using the values of K_{HCl} and Q listed in Table 2. It correlates the data well.

Table 2. Experimental Physical Properties of DIAION SA10A

Unit molecular structure	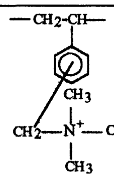	
Particle-size range (dry)	US standard mesh	24–28
Particle diameter (dry)	meter	6.756×10^{-4}
True density	kg of dry resin·m^{-3}	1.131
Saturation capacity of HCl, Q	mole·(kg dry resin)$^{-1}$	2.650
Equilibrium const. in Eq. 2, K_{HCl}	kg dry resin·mole^{-1}	9.060×10^2

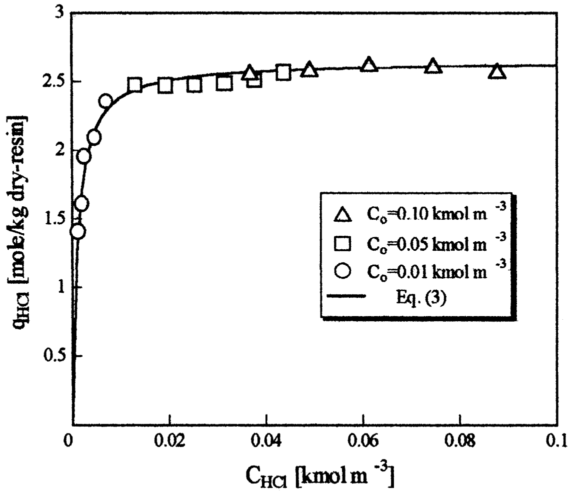

Figure 1. Experimental equilibrium isotherm of HCl on DIAION SA10A.

Results and Discussion

Figures 2–5 show the experimental equilibria for adsorption of PO$_4^{3-}$, HPO$_4^{2-}$, H$_2$PO$_4^-$, and H$_3$PO$_4$, respectively, ions on OH-type DIAION SA10A. In all the systems, the adsorption isotherms show a high amount of phosphate adsorption. Moreover, different behaviors in the adsorption

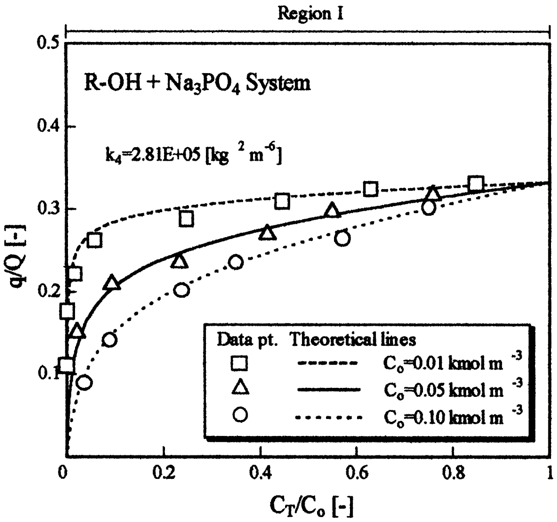

Figure 2. Experimental data vs. theoretical model for R-OH + Na$_3$PO$_4$ system.

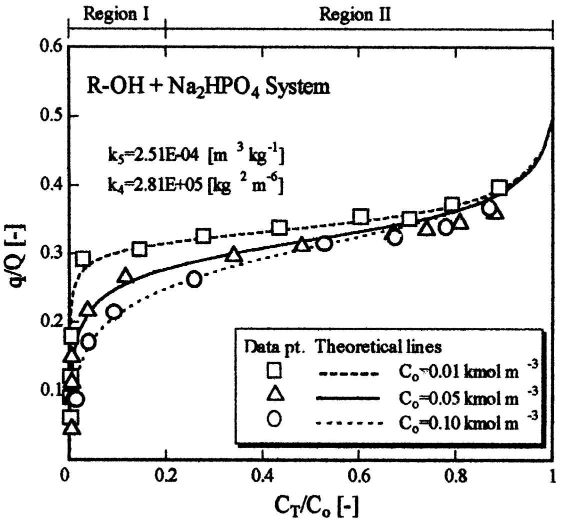

Figure 3. Experimental data vs. theoretical model for R-OH + Na_2HPO_4 system.

isotherms were observed. These peculiar behaviors were highly influenced by the pH of the equilibrated solutions.

In Figures 2–4, the initial concentrations of Na_3PO_4, Na_2HPO_4, and NaH_2PO_4 have a considerable effect on their experimental adsorption isotherms. At $C_T/C_o = 1.0$, the values of q/Q are 1, 1/2, and 1/3 for NaH_2PO_4, Na_2HPO_4, and Na_3PO_4, respectively.

In Figure 5, the experimental adsorption isotherm is not affected by the initial concentrations of H_3PO_4 solution. At an equilibrated solution concentration lower than about 5×10^{-5} kmol·m^{-3} the adsorption ratio is settling to a value of about 0.50, giving a flat-shaped curve. At this particular concentration range, this curve may be caused by the following ion-exchange reaction

$$2R\text{-}OH^- + H_2^+ HPO_4^{2-} \rightleftharpoons R_2\text{-}HPO_4^{2-} + 2H_2O \tag{5}$$

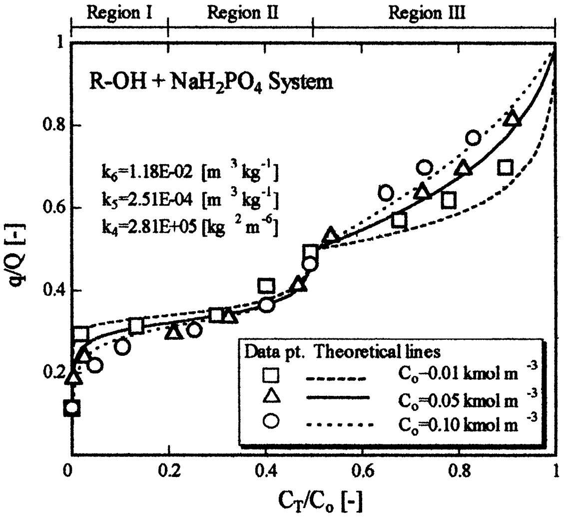

Figure 4. Experimental data vs. theoretical model for R-OH + NaH_2PO_4 system.

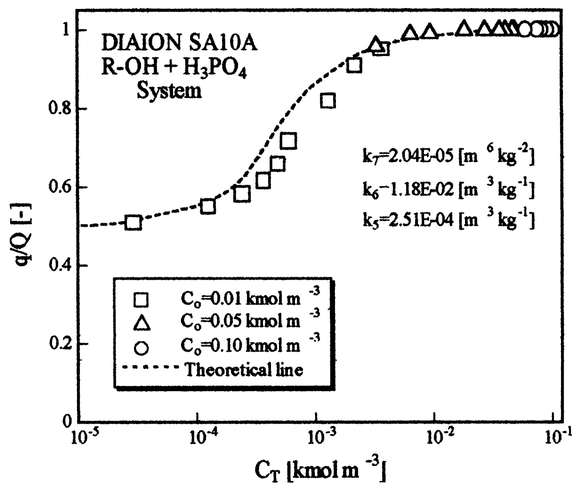

Figure 5. Experimental data vs. theoretical model for R-OH + H_3PO_4 system.

Moreover, the resin-phase concentration of phosphate ion increased with the increase in the equilibrated liquid-phase concentration. That is, there was a gradual increase of ion exchange for both HPO_4^{2-} and $H_2PO_4^-$ ions in the solution into the resin. At about 5×10^{-2} kmol·m^{-3} equilibrated concentration, the adsorption ratio reached $q/Q = 1.0$. At this juncture, the $H_2PO_4^-$ ion can be assumed to solely exist in the solution, as shown in the following ion-exchange reaction

$$R\text{-}OH^- + H^+ H_2PO_4^- \rightleftharpoons R\text{-}H_2PO_4^- + H_2O \tag{6}$$

In order to explain these peculiarities in the ion-exchange equilibria, a theoretical analysis for all equilibrium formation of ions in both the liquid and resin phases, is, therefore, proposed.

Equilibrium Formation of Phosphate Ions in the Liquid Phase

Considering a system where an OH-type strongly basic ion exchanger comes in contact with a $Na_xH_{3-x}PO_4$ aqueous solution ($x = 0, 1, 2, 3$), the dissociation equilibrium reaction of phosphate ion (PO_4^{3-}) is the same in all cases and only the x number of sodium ion (Na^+) differs. By applying the condition of electrical neutrality, one phosphate ion in a sodium phosphate molecule is generally taken as the number of sodium ion.

The different equilibrium reactions in the liquid phase are given by Eqs. 7 through 10, and the known dissociation constants (Musha, 1971) are summarized in Table 3.

$$H_3PO_4 \overset{k_1}{\rightleftharpoons} H^+ + H_2PO_4^- \tag{7}$$

$$H_2PO_4^- \overset{k_2}{\rightleftharpoons} H^+ + HPO_4^{2-} \tag{8}$$

$$HPO_4^{2-} \overset{k_3}{\rightleftharpoons} H^+ + PO_4^{3-} \tag{9}$$

$$H^+ + OH^- \overset{k_w}{\rightleftharpoons} H_2O \tag{10}$$

For simplicity, the mole concentrations [kmol·m^{-3}] of all ionic species in the liquid phase are represented by variables:

Table 3. Summary of Known and Determined Experimental Parameters

Known dissociation constants			
Equilibrium constant in Eq. 7	k_1	$\text{kmol}\cdot\text{m}^{-3}$	$7.52\ E-03$
Equilibrium constant in Eq. 8	k_2	$\text{kmol}\cdot\text{m}^{-3}$	$6.23\ E-08$
Equilibrium constant in Eq. 9	k_3	$\text{kmol}\cdot\text{m}^{-3}$	$4.80\ E-13$
Equilibrium constant in Eq. 10	k_w	$\text{kmol}\cdot\text{m}^{-3}$	$10.0\ E-14$
Determined experimental parameters			
Equilibrium constant in Eq. 25	k_4	$\text{kg}^2\cdot\text{m}^{-6}$	$2.81\ E+05$
Saturation capacity in Eq. 36	Q_T	$\text{mole}\cdot(\text{kg dry resin})^{-1}$	2.60
Equilibrium constant in Eq. 26	k_5	$\text{m}^3\cdot\text{kg}^{-1}$	$2.51\ E-04$
Saturation capacity in Eq. 43	Q_T	$\text{mole}\cdot(\text{kg dry resin})^{-1}$	2.34
Equilibrium constant in Eq. 27	k_6	$\text{m}^3\cdot\text{kg}^{-1}$	$1.18\ E-02$
Saturation capacity in Eq. 55	Q_T	$\text{mole}\cdot(\text{kg dry resin})^{-1}$	2.80
Equilibrium constant in Eq. 56	k_7	$\text{m}^6\cdot\text{kg}^{-2}$	$2.04\ E-05$

$A=[\text{Na}^+]$; $N=[\text{H}_3\text{PO}_4]$; $J=[\text{H}_2\text{PO}_4{}^-]$; $B=[\text{HPO}_4{}^{2-}]$; $P=[\text{PO}_4{}^{3-}]$; $F=[\text{H}^+]$; $G=[\text{OH}^-]$

By applying the mass action law, the preceding equations of equilibrium reactions are expressed as follows

$$k_1=\frac{[\text{H}^+][\text{H}_2\text{PO}_4{}^-]}{[\text{H}_3\text{PO}_4]}=\frac{F\cdot J}{N} \tag{11}$$

$$k_2=\frac{[\text{H}^+][\text{HPO}_4{}^{2-}]}{[\text{H}_2\text{PO}_4{}^-]}=\frac{F\cdot B}{J} \tag{12}$$

$$k_3=\frac{[\text{H}^+][\text{PO}_4{}^{3-}]}{[\text{HPO}_4{}^{2-}]}=\frac{F\cdot P}{B} \tag{13}$$

$$k_w=[\text{H}^+][\text{OH}^-]=F\cdot G \tag{14}$$

The total phosphate ion concentration C_T [$\text{kmol}\cdot\text{m}^{-3}$] in the equilibrated solution is defined by Eq. 15

$$C_T=N+J+B+P \tag{15}$$

In addition, the electrical neutrality condition is given by Eq. 16

$$A+F=J+2B+3P+G \tag{16}$$

where A is related to the total concentration of phosphate ($\text{Na}_x\text{H}_{3-x}\text{PO}_4$), expressed by Eq. 17

$$A=xC_T \tag{17}$$

Meanwhile, Eq. 14 is rearranged into Eq. 18

$$F=\frac{k_w}{G} \tag{18}$$

When Eqs. 17 and 18 are substituted to Eq. 16, Eq. 19 is derived

$$xC_T+\frac{k_w}{G}=J+2B+3P+G \tag{19}$$

Moreover, when Eqs. 13 and 18 are combined, B is obtained

$$B=\frac{k_wP}{k_3G} \tag{20}$$

Then J is derived from Eq. 12 with Eqs. 18 and 20

$$J=\frac{k_w{}^2P}{k_2k_3G^2} \tag{21}$$

On the other hand, N is obtained by substituting Eqs. 18 and 21 into Eq. 11

$$N=\frac{k_w{}^3P}{k_1k_2k_3G^3} \tag{22}$$

Therefore, P is derived from Eq. 15 when Eqs. 20, 21, and 22 are combined

$$P=\frac{C_T}{\dfrac{k_w}{k_3G}+\dfrac{k_w{}^2}{k_2k_3G^2}+\dfrac{k_w{}^3}{k_1k_2k_3G^3}+1} \tag{23}$$

Finally, Eq. 19 is wholly transformed into Eq. 24

$$xC_T+\frac{k_w}{G}-\frac{k_w{}^2P}{k_2k_3G^2}-\frac{2k_wP}{k_3G}-3P-G=0 \tag{24}$$

The values of P and G are determined by solving Eqs. 23 and 24 simultaneously. Consequently, the values of B, J, N, and F are also obtained.

Theoretical Analysis in the Adsorption Isotherms

Equilibrium relationship between R–OH and sodium phosphate compounds

For the system $\text{R–OH}+\text{Na}_x\text{H}_{3-x}\text{PO}_4$ ($x=1$, 2, 3), the equations of ion-exchange reactions at different ion formations in the resin phase are given by Eqs. 25–27

$$3\text{R}-\text{OH}^-+\text{PO}_4{}^{3-}\xrightleftharpoons{k_4}\text{R}_3-\text{PO}_4{}^{3-}+3\text{OH}^- \tag{25}$$

$$2\text{R}_3-\text{PO}_4{}^{3-}+3\text{HPO}_4{}^{2-}\xrightleftharpoons{k_5}3\text{R}_2-\text{HPO}_4{}^{2-}+2\text{PO}_4{}^{3-} \tag{26}$$

$$\text{R}_2-\text{HPO}_4{}^{2-}+2\text{H}_2\text{PO}_4{}^-\xrightleftharpoons{k_6}2\text{R}-\text{H}_2\text{PO}_4{}^-+\text{HPO}_4{}^{2-} \tag{27}$$

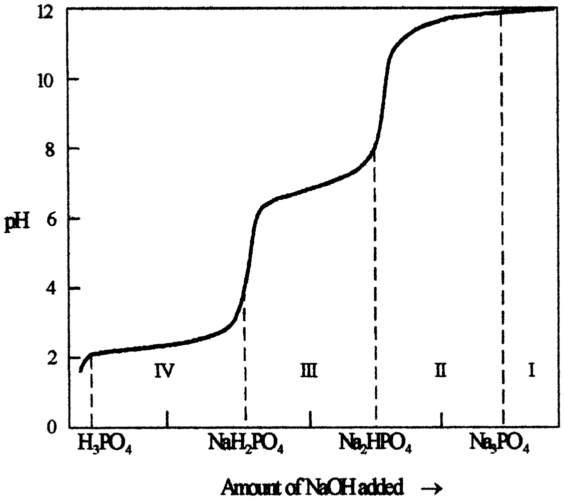

Figure 6. Titration curve of H_3PO_4 with NaOH.

Again for simplicity, the mole concentrations [mole·(kg dry resin)$^{-1}$] of all ionic species in the resin phase are assigned by variables: $c = [\text{R-OH}^-]$; $d = [\text{R}_3\text{-PO}_4^{3-}]$; $e = [\text{R}_2\text{-HPO}_4^{2-}]$; $r = [\text{R-H}_2\text{PO}_4^-]$.

The unknown experimental equilibrium constants k_4, k_5, and k_6 in the preceding equations are determined by using the following procedure: Figure 6 shows a titration curve of H_3PO_4 with NaOH (Morino, 1973). The curve is divided into four distinct regions. At pH > 12 (designated as Region I), only the PO_4^{3-} ion exists. At 8 < pH < 12 (Region II), both the HPO_4^{2-} and PO_4^{3-} ions coexist. At 4 < pH < 8 (Region III), both the $H_2PO_4^-$ and HPO_4^{2-} ions coexist. And at pH < 4 (Region IV), only the $H_2PO_4^-$ ion exists.

Region I model: Adsorption of tribasic phosphate

In Region I, since only the PO_4^{3-} ion is involved in the ion-exchange reaction, the equilibrium ion-exchange reaction is given by Eq. 25. By applying the mass action law to Eq. 25, the equilibrium constant k_4 is expressed by Eq. 28

$$k_4 = \frac{dG^3}{c^3 P} \tag{28}$$

The total phosphate ion concentration in the equilibrated solution C_T [kmol·m^{-3}], the total phosphate ion concentration in the resin phase q [mole·(kg dry resin)$^{-1}$], and the saturation capacity of the resin Q_T [mole·(kg dry resin)$^{-1}$] are given as follows

$$C_T = P \tag{29}$$

$$q = d \tag{30}$$

$$Q_T = 3d + c \tag{31}$$

The parameter c is obtained by combining Eqs. 30 and 31

$$c = Q_T - 3q \tag{32}$$

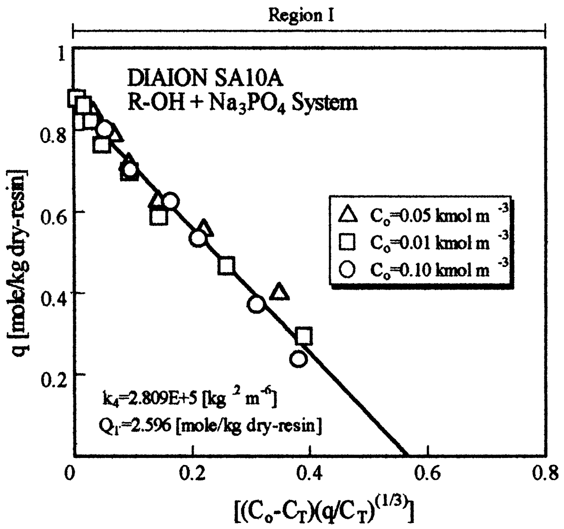

Figure 7. k_4 determination (Eq. 36).

Hence, Eq. 28 is partially expressed by Eq. 33

$$k_4 = \frac{G^3 q}{(Q_T - 3q)^3 C_T} \tag{33}$$

By the condition of electrical neutrality in the liquid phase, G is given by Eq. 34

$$G = 3(C_0 - C_T) \tag{34}$$

Thus, Eq. 33 is completely transformed into Eq. 35

$$k_4 = \frac{(3C_0 - 3C_T)^3 q}{(Q_T - 3q)^3 C_T} \tag{35}$$

When Eq. 35 is appropriately rearranged, Eq. 36 is obtained

$$q = -\left(\frac{1}{k_4}\right)^{1/3} (C_0 - C_T)\left(\frac{q}{C_T}\right)^{1/3} + \frac{Q_T}{3} \tag{36}$$

Figure 7 shows the plot of the experimental adsorption equilibrium data of R–OH + Na_3PO_4 system based on Eq. 36. The data are correlated well by the straight line. The values of the experimental equilibrium constant k_4 and the saturation capacity Q_T were determined from the slope and intercept of the line, respectively. The obtained values are listed in Table 3. The value of Q_T is slightly smaller than the exchange capacity, Q, determined from Figure 1. The theoretical lines in Figure 2 were calculated based on Eq. 35, using the values of the equilibrium constants given in Table 3. For all concentration ranges, it appeared that the data can be correlated by Eq. 35.

Adsorption of dibasic phosphate

Figure 3 shows the experimental adsorption isotherm of R–OH + Na_2HPO_4 system. It is divided into two distinct regions: Region I and Region II. In Region II, both the HPO_4^{2-}

and PO_4^{3-} ions are involved in the ion-exchange reactions. That is, when an OH^--type resin is added to the Na_2HPO_4 solution, HPO_4^{2-} is exchanged for OH^- in the resin phase. Then the concentration of OH^- ions in the liquid phase is increased and the pH of the solution is also increased. Thus, HPO_4^{2-} ions are partly converted to PO_4^{3-} ions and the exchange reactions of Eqs. 25 and 26 occur in Region I in Figure 3. When OH^- ions in the resin phase are completely consumed by the ion-exchange reactions, only the ion exchange in Eq. 26 occurs (Region II in Figure 3). The relation between the experimental pH values and the resin-phase concentration of phosphate supported the preceding explanation. The two equilibrium models are discussed in more detail as they occur.

Region II model

As discussed earlier, only the ion-exchange reaction of Eq. 26 is involved in this Region II in Figure 3. By applying the mass action law to Eq. 26, the equilibrium constant k_5 is given by Eq. 37

$$k_5 = \frac{e^3 P^2}{d^2 B^3} \tag{37}$$

At this particular ion-exchange reaction, the total phosphate ion concentration in the resin phase, q, and the saturation capacity of the resin Q_T are expressed by the following equations

$$q = e + d \tag{38}$$

$$Q_T = 2e + 3d \tag{39}$$

The relationship between q and Q_T as expressed in terms of e and d is easily derived from Eqs. 38 and 39

$$e = 3q - Q_T \tag{40}$$

$$d = Q_T - 2q \tag{41}$$

Then Eq. 37 is transformed into Eq. 42

$$k_5 = \frac{(3q - Q_T)^3 P^2}{(Q_T - 2q)^2 B^3} \tag{42}$$

Thus, the equation for the unknown equilibrium constant k_5 is obtained

$$q = k_5^{1/3} \frac{B}{3} \left(\frac{Q_T - 2q}{P} \right)^{2/3} + \frac{Q_T}{3} \tag{43}$$

Figure 8 shows the plot of all the experimental adsorption equilibrium data of the $R\text{-}OH + Na_2HPO_4$ system based on Eq. 43. The values of B and P were calculated using Eqs. 20 and 23, respectively. The value of the exchange capacity Q in Table 2 was initially used as Q_T. When the value of the transverse axis is larger than about 0.03, the plots are correlated by a straight line. This means that in this particular region, only the ion-exchange reaction in Eq. 26 occurs. The value of k_5 was determined from the slope of the straight line and Q_T was calculated from the intercept. These values are listed in Table 3. In Figure 3, the theoretical lines in Region II were all calculated based on Eq. 42, since only its contribution is significant in this particular region. The theoretical lines in Region I were all obtained by the following analysis.

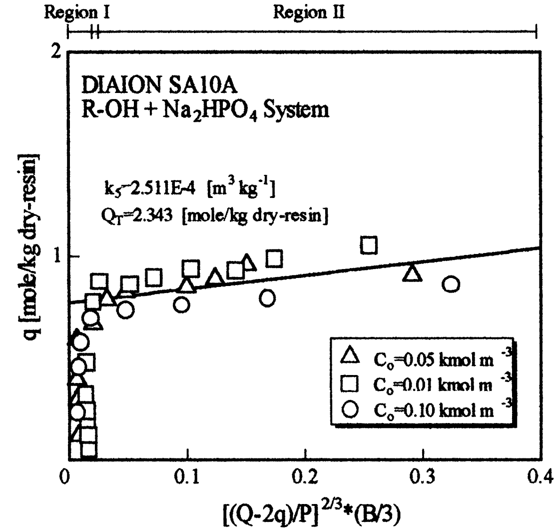

Figure 8. k_5 determination (Eq. 43).

Region I model

In order to account for the possible existence of HPO_4^{2-} ions in Region I, a new equilibrium model for Region I for this particular system is proposed. In this analysis, the equilibrium ion-exchange reactions in Eqs. 25 and 26 are both considered. The corresponding unknown experimental equilibrium constants were given previously by Eqs. 28 and 37, respectively. Therefore, the total phosphate ion concentration in the resin phase, q, and the saturation capacity of the resin, Q_T, are given by Eqs. 38 and 44, respectively

$$Q_T = c + 3d + 2e \tag{44}$$

By combining these equations, d and e are easily obtained

$$d = Q_T - c - 2q \tag{45}$$

$$e = 3q - Q_T + c \tag{46}$$

Substituting Eq. 45 into Eq. 28 yields a new expression of k_4 given by Eq. 47

$$k_4 = \frac{(Q_T - c - 2q) G^3}{c^3 P} \tag{47}$$

And by substituting Eqs. 45 and 46 into Eq. 37, a new expression of k_5 is obtained

$$k_5 = \frac{(3q - Q_T + c)^3 P^2}{(Q_T - c - 2q)^2 B^3} \tag{48}$$

The unknown parameters c and q were determined by solving Eqs. 47 and 48 simultaneously, using the previously obtained values of k_4 and k_5 in Table 3. The value of Q in Table 2 was initially used as Q_T. Similarly, the values of the parameters B, P, and G were calculated from Eqs. 20, 23, and 24, respectively. The theoretical lines of Region I in Figure 3 were all calculated based on Eqs. 47 and 48.

Adsorption of monobasic phosphate

For the R−OH + NaH$_2$PO$_4$ system, the phosphate ions $H_2PO_4^-$, HPO_4^{2-}, and PO_4^{3-} are all involved in the ion-exchange reactions. Figure 4 shows the experimental adsorption isotherm with three divisions: Regions I, II, and III. At first, when an OH$^-$-type resin is added to the NaH$_2$PO$_4$ solution, $H_2PO_4^-$ is exchanged for OH^- in the resin phase. When OH^- coexists in the resin phase ($q/Q <$ about 1/3), the pH of the solution showed the value in Region I. That is, ion-exchange reactions Eqs. 25 and 26 may occur in $q/Q <$ about 1/3. In the region where about $1/3 < q/Q < 1/2$, the pH of the solution showed the value of Region II. In this region, the ion-exchange reaction is expressed by Eq. 26. When q/Q is larger than about 0.5, the pH of the solution showed the value in Region III. Thus, the ion-exchange reaction in this particular region is given by Eq. 27. The Region I and Region II models were discussed in the preceding sections.

Region III model

The Region III equilibrium model is based on Eq. 27. Likewise, the equation for the unknown experimental equilibrium constant, k_6, is obtained by applying the mass action law to Eq. 27

$$k_6 = \frac{r^2 B}{eJ^2} \tag{49}$$

In this particular region, the total phosphate ion concentration in the resin phase, q, and the saturation capacity of the resin Q_T are expressed as follows

$$q = r + e \tag{50}$$

$$Q_T = r + 2e \tag{51}$$

Similarly, e and r are easily determined from the preceding equations

$$e = Q_T - q \tag{52}$$

$$r = 2q - Q_T \tag{53}$$

Hence, k_6 is obtained by appropriate substitutions into Eq. 49

$$k_6 = \frac{(2q - Q_T)^2 B}{(Q_T - q)J^2} \tag{54}$$

Then q is derived from Eq. 54, which is given by Eq. 55

$$q = k_6^{1/2}\frac{J}{2}\left(\frac{Q_T - q}{B}\right)^{1/2} + \frac{Q_T}{2} \tag{55}$$

Parameters B and J were calculated using Eqs. 20 and 21, respectively. The value of Q in Table 2 was initially used as Q_T. Figure 9 shows the plot of the experimental equilibrium data of the R-OH + NaH$_2$PO$_4$ system based on Eq. 55. When the value of the transverse axis is larger than about 0.01, the plots are correlated by a straight line. This means that in this particular region, only the ion-exchange reaction in Eq. 27 occurs, which is Region III. The unknown experimental equilibrium constant k_6 was determined from the slope of the straight line using only the data under Region III, since only the contribution of Eq. 54 is significant in this particular region. The intercept of the straight line gave the value of Q_T. The obtained values of k_6 and Q_T are listed in Table 3.

In Figure 4, the theoretical lines under Region III ($C_T/C_o \geq 0.50$) were obtained based on Eq. 54. However, the equation became insignificant under Region II ($C_T/C_o \leq 0.50$), since it could no longer give a good correlation of the experimental adsorption data in the region, as shown in Figure 9. Therefore, Eq. 42 was used to obtain the theoretical lines in Region II. The obtained results were consistent with Figure 3, where the maximum adsorption ratio is 0.50. However, Eq. 42 became insignificant under Region I ($C_T/C_o \leq 0.20$). Thus, as explained earlier, Eqs. 47 and 48 were used to determine the theoretical lines in Region I.

Equilibrium model for OH-type resin and H_3PO_4 system

In the equilibrium relationship of the R−OH + H$_3$PO$_4$ system, when $q/Q <$ about 1/3, OH^- in the resin phase is exchanged for $H_2PO_4^-$ according to Eq. 25, as shown in the preceding cases. In this particular system, since the cation in the liquid phase is only H^+, the OH^- in the liquid phase is consumed by the instantaneous reaction expressed by Eq. 10. Therefore, in the experimental condition shown in Figure 5, that is, $q/Q > 0.5$, the ion-exchange reactions given by Eqs. 26, 27, and 56 are considered.

$$R_3-PO_4^{3-} + 3H_2PO_4^- \overset{k_7}{\rightleftarrows} 3R-H_2PO_4^- + PO_4^{3-} \tag{56}$$

The equilibrium constants k_5 and k_6 are given by Eqs. 37 and 49, respectively while the equilibrium constant k_7 is expressed by Eq. 57

$$k_7 = \frac{r^3 P}{dJ^3} \tag{57}$$

The total phosphate ion concentration in the resin phase, q, and the total ion-exchange capacity of the resin, Q_T, are defined by Eqs. 58 and 59

$$q = d + e + r \tag{58}$$

$$Q_T = 3d + 2e + r \tag{59}$$

When the preceding two equations are combined, the parameters e and r are obtained

$$e = Q_T - q - 2d \tag{60}$$

$$r = 2q - Q_T + d \tag{61}$$

Then substituting Eqs. 60 and 61 into Eq. 49 and rearranging, the parameter d is derived

$$d=\frac{-\left[2B(2q-Q_T)+2k_6J^2\right]+\sqrt{\left[2B(2q-Q_T)+2k_6J^2\right]^2-4B\left[B(2q-Q_T)^2-k_6J^2(Q_T-q)\right]}}{2B} \tag{62}$$

In addition, a new expression of k_5 and k_7 is obtained when r in Eq. 61 is replaced in both Eqs. 37 and 57

$$k_5=\frac{(Q_T-q-2d)^3P^2}{d^2B^3} \tag{63}$$

$$k_7=\frac{(2q-Q_T+d)^3P}{dJ^3} \tag{64}$$

Therefore, k_7 can be determined by solving Eqs. 57 and 58 simultaneously. It can also be easily calculated from the previously determined values of k_5 and k_6 based on Eq. 65

$$k_7=\left(k_6^3k_5\right)^{1/2} \tag{65}$$

Figure 5 shows the plot of the experimental equilibrium data and the calculated theoretical line of the R–OH+H_3PO_4 system based on Eqs. 62–64. The unknown experimental equilibrium constant k_7 was determined from Eq. 65. It appears that the data can be correlated for all concentration ranges by these equations. The experimental data show a slight deviation from the theoretical line at around a 5×10^{-4} to 1×10^{-3} kmol·m^{-3} concentration range. The slight difference is considered to be an effect of the k_7 value, which was obtained from the calculated experimental equilibrium constants of the R–OH+NaH_2PO_4 and R–OH+Na_2HPO_4 systems. Apparently, the value of k_7 depends greatly on the accuracy of k_5 and k_6 values.

In all the systems considered, the proposed theoretical models were able to correlate the experimental equilibrium data well. Also, the peculiar behaviors in the obtained experimental adsorption isotherms are explained.

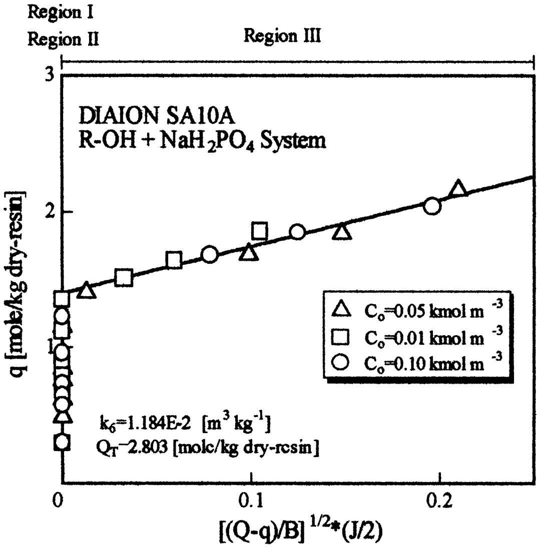

Figure 9. k_6 determination (Eq. 55).

Conclusions

An experimental study on the equilibrium isotherms for adsorption of H_3PO_4, $H_2PO_4^-$, HPO_4^{2-}, and PO_4^{3-} ions using an OH-type strongly basic ion exchanger, DIAION SA10A, in aqueous media and at wide pH ranges was conducted. This fundamental study is aimed at understanding the basic ion-exchange mechanism of phosphates in this type of ion exchanger, to clearly elucidate the ion-exchange behavior of phosphates, and to establish working equilibrium models that could possibly lead to the development of an adsorption-recovery technology for phosphates. The adsorption of phosphate ions using OH-type resin appeared technically feasible.

In all the systems considered, the experimental adsorption isotherms showed a high amount of phosphate adsorption. This is explained by the apparently high values of the saturation capacities of the resin obtained for all the systems considered, as compared to the total ion-exchange capacity of the resin. Except in the H_3PO_4 system, all adsorption isotherms were affected by the initial concentrations of the solutions and exhibited different adsorption behaviors for all phosphate ions. These peculiar behaviors were greatly influenced by the pH of the equilibrated solutions. By applying the mass action law to the dissociation reactions in the liquid phase and ion-exchange reactions, the theoretical equations for the adsorption isotherms were derived. In this study, the proposed ion-exchange reaction models were able to correlate the experimental data for adsorption of H_3PO_4, NaH_2PO_4, Na_2HPO_4, and Na_3PO_4 well, and explained the peculiarities in the obtained experimental adsorption isotherms.

These derived experimental equilibrium models will be tested further in the next stage of this study by considering other competing ions, such as chloride, sulfate, calcium, nitrate, to determine the commercial feasibility of the OH-type anion exchanger.

Notation

A = mole concentration of Na^+ ion in the liquid phase, kmol·m^{-3}
B = mole concentration of HPO_4^{2-} ion in the liquid phase, kmol·m^{-3}
C_o = initial phosphate concentration in the unequilibrated solution, kmol·m^{-3}
C_T = total phosphate concentration in the equilibrated solution, kmol·m^{-3}
c = mole concentration of OH^- ion in the resin phase, mole·(kg dry resin)$^{-1}$
d = mole concentration of PO_4^{3-} ion in the resin phase, mole·(kg dry resin)$^{-1}$
e = mole concentration of HPO_4^{2-} ion in the resin phase, mole·(kg dry resin)$^{-1}$
F = mole concentration of H^+ ion in the liquid phase, kmol·m^{-3}
G = mole concentration of OH^- ion in the liquid phase, kmol·m^{-3}

J = mole concentration of HPO_4^{2-} ion in the liquid phase, $kmol \cdot m^{-3}$

k_w = known dissociation constant of water in Eq. 10, $(kmol \cdot m^{-3})^2$

k_1 = known dissociation constant of phosphate in Eq. 7, $kmol \cdot m^{-3}$

k_2 = known dissociation constant of phosphate in Eq. 8, $kmol \cdot m^{-3}$

k_3 = known dissociation constant of phosphate in Eq. 9, $kmol \cdot m^{-3}$

k_4 = experimental equilibrium constant in Eq. 25, $kg^2 \cdot m^{-6}$

k_5 = experimental equilibrium constant in Eq. 26, $m^3 \cdot kg^{-1}$

k_6 = experimental equilibrium constant in Eq. 27, $m^3 \cdot kg^{-1}$

k_7 = experimental equilibrium constant in Eq. 56, $m^6 \cdot kg^{-2}$

N = mole concentration of H_3PO_4 ion in the liquid phase, $kmol \cdot m^{-3}$

P = mole concentration of PO_4^{3-} ion in the liquid phase, $kmol \cdot m^{-3}$

Q = total ion-exchange capacity of the resin, $mole \cdot (kg\ dry\ resin)^{-1}$

Q_T = saturation capacity of the resin (Eqs. 36, 43, 44, 55, and 59), $mole \cdot (kg\ dry\ resin)^{-1}$

q = total phosphate ion concentration in the resin phase, $mole \cdot (kg\ dry\ resin)^{-1}$

r = mole concentration of $H_2PO_4^{-}$ ion in the resin phase, $mole \cdot (kg\ dry\ resin)^{-1}$

x = ratio number of sodium ion to phosphate ion in a sodium phosphate molecule

Literature Cited

Aotani, K., *Gou Mikki: Kinzoku Mikki Gijutsu 2* (*Alloy Plating: Metal Plating Technology 2*), Maki Shoten, Tokyo, Japan (1966).

Asahara, S., *Kinzoku Hyoumen Gijutsu Benran* (*Metal Surface Technology Handbook*), Nikkan Kougyou Shinbunsha, Tokyo, Japan (1976).

Boki, K., and S. Tanada, "Phosphate Removal by Adsorption to Activated Carbon," *Jpn. J. Hygiene*, **42**, 710 (1987).

Considine, D. M., *Van Nostrand Reinhold Encyclopedia of Chemistry*, 4th ed., Van Nostrand Reinhold, New York, p. 709 (1984).

Elvers, B., S. Hawkins, and G. Schulz, "Metals, Surface Treatment: Phosphating," *Ullman's Encyclopedia of Industrial Chemistry*, Vol. A16, 5th ed., VCH, Weinheim, Germany, p. 411 (1990).

Elvers, B., S. Hawkins, and G. Schulz, "Phosphoric Acid and Phosphates," *Ullman's Encyclopedia of Industrial Chemistry*, VCH, Weinheim, Germany, Vol. A19, 5th ed., p. 480 (1991).

Japanese Industrial Standards, JIS K 9007, Japanese Standards Association, Tokyo (1996).

Jenkins, D., and S. W. Hermanowics, "Principles of Chemical Phosphate Removal," *Phosphorus and Nitrogen Removal from Municipal Wastewater: Principles and Practice*, 2nd ed., R. I. Sedlak, ed., H. K. Lewis, London, p. 91 (1991).

Kirk, R. E., D. F. Othmer, M. Grayson, and D. Eckroth, "Metal Surface Treatments (Chemical)," *Kirk-Othmer Encyclopedia of Chemical Technology*, Vol. 15, 3rd ed., Wiley, New York p. 304 (1981).

Morino, Y., *Kagaku Benran Ouyouhen* (*Chemical Handbook Application*), 2nd ed., Maruzen Kabushiki Gaisha, Tokyo, p. 158 (1973).

Musha, S., *Bunseki Kagaku Jiten* (*Analytical Chemistry Dictionary*), Kyoritsu Shuppan Kabushiki Gaisha, Tokyo, p. 1992 (1971).

Ogawa, T., "Phosphorous Removal from Effluents Discharged from Night-Soil Treatment Plants (in Japanese)," *Yosui to Housui (Irrigation Water and Wastewater)*, **22**, 964 (1980).

Sengupta, A. K., and D. Zhao "Selective Removal of Phosphates and Chromates from Contaminated Water by Ion Exchange," U.S. Patent No. 6,136,199 (2000).

Stensel, H. D., "Principles of Biological Phosphorus Removal," *Phosphorus and Nitrogen Removal from Municipal Wastewater: Principles and Practice*, 2nd ed., R. I. Sedlak, ed., H. K. Lewis, London, p. 141 (1991).

Tanasheva, M. R., M. S. Kazymbetova, S. B. Gunter, D. A. Smagulova, R. S. Makhatova, and U. D. Dzusipbekov, "An Ion-exchange Extraction of Valuable Components Out of Wastewaters," *Ion Exch. Adv. Proc. IEX '92*, p. 302 (1992).

Urano, K., and H. Tachikawa, "Process Development for Removal and Recovery of Phosphorus from Wastewater by a New Adsorbent. 1. Preparation Method and Adsorption Capability of a New Adsorbent," *Ind. Eng. Chem. Res.*, **30**, 1893 (1991).

Zhao, D., and A. K. Sengupta, "Selective Removal and Recovery of Phosphate in a Novel Fixed-Bed Process," *Water Sci. Technol.*, **33**, 139 (1996).

Zhao, D., and A. K. Sengupta, "Ultimate Removal of Phosphate from Wastewater Using a New Class of Polymeric Ion Exchangers," *Water Res.*, **32**, 1613 (1998).

Manuscript received July 24, 2001, and revision received Feb. 20, 2002.